Colloidal Membranes

Lecture Series: Colloidal Phenomena

AGENDA

1. Introduction/Disambiguation
2. Membranes by surfactant self-assembly
3. Polymeric membranes
4. Summary

Introduction

- Main discrimination possible between:
  - Natural (biological) vs. Artificial (man-made) membranes

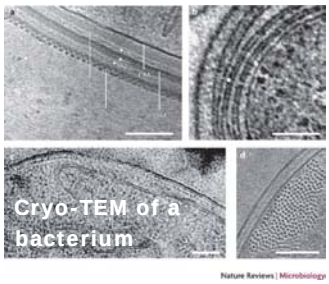

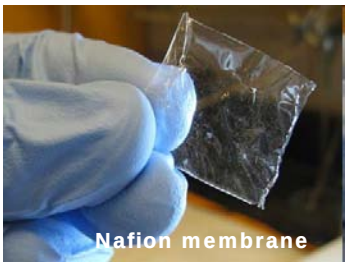

- Further discrimination on the basis of transport properties, material properties (surfactants, polymers, etc.), pore sizes, etc.

Unifiying concept: **Separation of compartments!**

Membranes by surfactant self-assembly

Reminder:

Amphiphilic molecules
→ Self-assembly in aqueous solution

Different morphologies:
spherical micelles (a)
worm-like micelles (e)
vesicles (d)
bilayers (c)

Driving force: hydrophobic effect
→ exclusion of hydrophobic part from water to minimize water contact

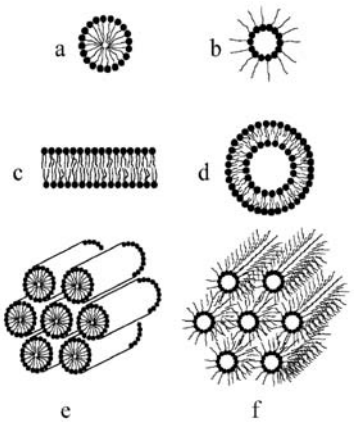

Figure 2 Common lamellar and nonlamellar self-assembled structures of lipids: (*a*) micelle, (*b*) inverse micelle, (*c*) lamellar bilayer, (*d*) bilayer vesicle, (*e*) hexagonal, (*f*) inverse hexagonal.

Membranes by surfactant self-assembly
packing parameter

form of an aggregate is determined by the surfactant geometry

universal validity:
low molecular weight surfactants → amphiphilic block copolymers

Other factors:

polarity

chain: length, branching, flexibility

charge

concentration

temperature

Geometical Contribution

v = volume of molecule, a = area of polar head group, l = length of HC chain

LIPIDS	LIPID SHAPE	ORGANIZATION	PHASE
Soaps, detergents	Inverted cone P< 1/3-2/3	Micelles	Isotropic hexagonal I
Phosphotidyl choline	Cylinder P~1	Bilayer	Lamellar (cubic)
Phosphatidyl-ethanolamine	Cone P> 1	Reverse micelle	Reverse micelle, hexagonal II
Mixtures	P~ 1	Bilayer	lamellar

Lipids

- membrane lipids are the building blocks of natural bilayer systems

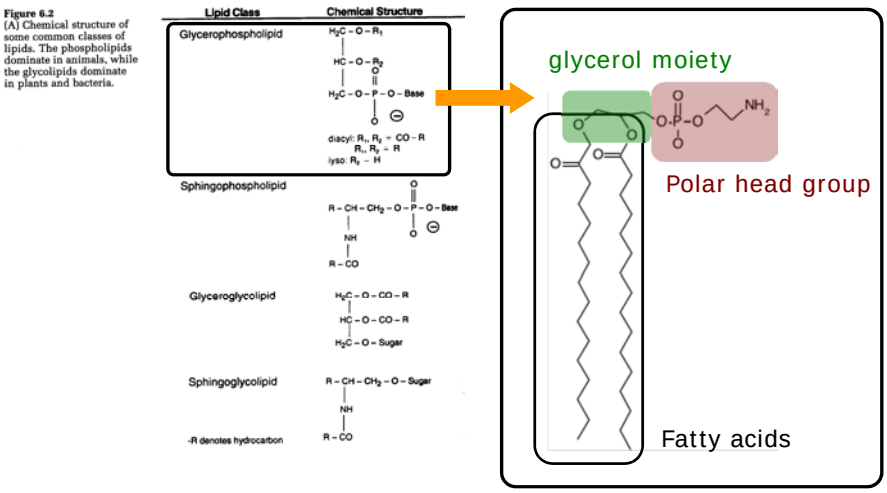

Bilayer membranes

- approaches to achieve $P = v/(l*a_0) \approx 1$

small headgroup and/or **bulky apolar tails**

- Two alkyl chains instead of one

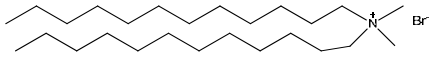

vs.

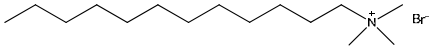

- smaller headgroups (size reduction in case of nonionic surfactants, introduction of cosurfactants with very small headgroups (e.g. addition of alkanols like decanol)

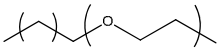

$C_{12}E_4$ forms lamellae at room temperature
$C_{12}E_5$ forms lamellae at 50°C

Lipids

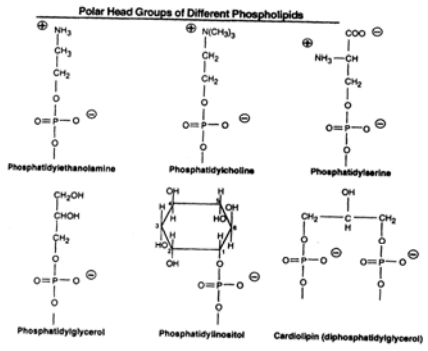

TABLE 6.1 Common Name of Acyl Chains and Melting Point of the Corresponding Fatty Acid

Acyl Chain	*Common Name*	*Symbol*	*Melting Point of Acid (°C)*
$CH_3(CH_2)_6-C(=O)-O-$	capryl	8:0	16
$CH_3(CH_2)_8-C(=O)-O-$	capric	10:0	32
$CH_3(CH_2)_{10}-C(=O)-O-$	lauroyl	12:0	44
$CH_3(CH_2)_{12}-C(=O)-O-$	myristoyl	14:0	54
$CH_3(CH_2)_{14}-C(=O)-O-$	palmitoyl	16:0	63
$CH_3(CH_2)_{16}-C(=O)-O-$	stearoyl	18:0	70
$CH_3(CH_2)_{18}-C(=O)-O-$	arachidoyl	20:0	77
$CH_3(CH_2)_7-CH=CH-(CH_2)_7-C(=O)-O-$	oleoyl	$18:1^{\Delta 9}$	13
$CH_3(CH_2)_4-CH=CH-CH_2-CH=CH-(CH_2)_6-C(=O)-O-$	linoleoyl	$18:2^{\Delta 9,12}$	−5
$CH_3CH_2-CH=CH-CH_2-CH=CH-CH_2-CH=CH-(CH_2)_6-C(=O)-O-$	linolenoyl	$18:3^{\Delta 9,12,15}$	−11
$CH_3(CH_2)_4-CH=CH-CH_2-CH=CH-CH_2-CH=CH-CH_2-CH=CH-(CH_2)_2-C(=O)-O-$	arachidonoyl	$20:4^{\Delta 5,8,11,14}$	−50

Bilayer formation vs. Micelle formation

TABLE 6.3 Comparison Between Properties of Micellar and Bilayer Aggregates

Property	*Micelles*	*Bilayers*
Monomer solubility	$\sim 10^{-2}$ M	10^{-5}–10^{-10} M
τ for monomer exchange	10^{-3}–10^{-6} s	10^{2}–10^{-3} s
τ for aggregate lifetime	10^{-1}–10^{-3} s	days to years
Characteristic temperature	Krafft temperature	Chain-melting temperature
Structural directionality	All directions equivalent	Lateral diffusion rapid, flip-flop slow
Aggregation pattern	Forms well-defined aggregate at well-defined CMC	Basic structural unit appears in a variety of global structures

- Micelles will not grow in size but in number upon surfactant addition
- Idealistic: No molecular limit for bilayer growth in lateral direction
  → but line tension will force defects or closure: vesicles!

vesicles

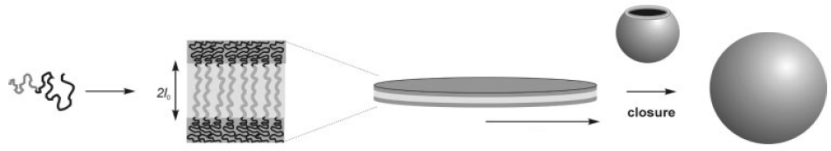

Planar bilayer:
problem: # edges in contact with water
→ increase of line energy (E_{disk}) – surface tension along the circular rim

Vesicular structure:
problem: # bending of the bilayer
→ deformation of amphiphiles (E_{bend})

vesicles

Uni-lamellar vesicle

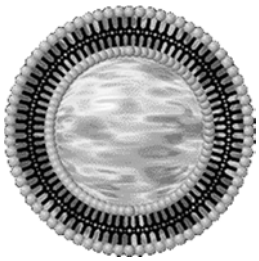

Multi-lamellar vesicle

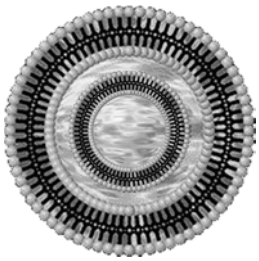

SUV (small unilamellar vesicle): ~ 20 nm

LUV (large unilamellar vesicle): ~ 100 nm

GUV (giant unilamellar vesicle): ~ 1-100 μm

Sizes, type and polydispersity depend also on preparation!

Inner Structure of Bilayer Systems

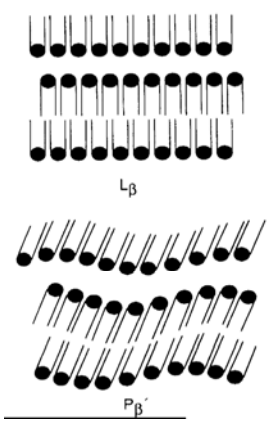

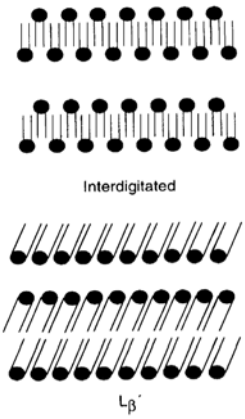

Figure 6.3
When alkyl chains crystallize, they have a cross-sectional area of ≈20 Å² per chain in a plane perpendicular to the direction of the chain. If the area of the polar groups in the bilayer matches that of the chain(s), a structure L_β is adopted. In the more likely case of a mismatch between polar head and chain areas, a tilted structure, as in $L_{\beta'}$, or a rippled structure, as in $P_{\beta'}$, can appear. For single-chain amphiphiles, chains may even interdigitate, making the thickness of the apolar layer the same as the length of a single chain.

How was this picture developed?

Characterization of bilayer systems

- Complete characterisation requires use of multiple techniques:
  - X-ray or Neutron diffraction (lamellae size, repeat unit, …)
  - Microscopy (vesicle size, morphology)
  - Light Scattering methods (vesicle size, shape)
  - Nuclear Magnetic Resonance spectroscopy (molecular level structure)
  - Calorimetry (phase transitions, enthalpies, etc.)
  - …many more techniques are available

Diffraction

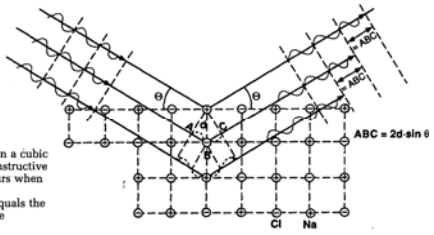

Figure 6.5
Bragg reflection in a cubic NaCl crystal. Constructive interference occurs when the distance $ABC = 2d \sin\theta$ equals the wavelength of the radiation.

gure 6.6
presentation of a mellar phase with a peat distance d in terms pairs of layers of ickness d_1 and d_2 ntaining solvent and mphiphile, respectively. ith a total lamellar area of , the total volume $= dA$, and the volumes of e respective regions are $A = V_i = n_i v_i$, where n_i quals the amount and v_i e partial molar volume. liminating the area A, we nd $d_i = d(1 + n_1 v_1 / [n_2 v_2])^{-1}$.

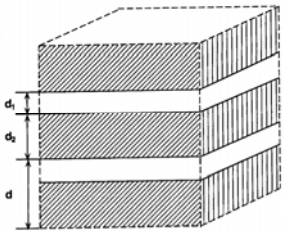

Figure 6.7
Double logarithmic plot of repeat distance (Å) versus inverse amphiphile volume fraction $\Phi_a = n_2 v_2 / (n_1 v_1 + n_2 v_2)$ for CTAB–hexanol–water (molar ratio 2.38:1). The straight lines have a slope of 1.0, showing that $d \sim \Phi_a^{-1}$, which is characteristic for one-dimensional swelling. (K. Fontell, A. Khan, D. Maciejewska, and S. Puang, *Colloid Polym. Sci.* **269**, 727 (1991).)

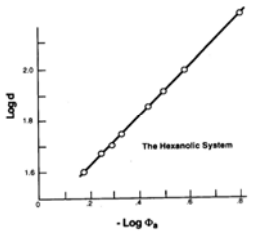

Calorimetry

THE JOURNAL OF BIOLOGICAL CHEMISTRY
Vol. 247, No. 19, Issue of October 10, pp. 6071–6075, 1972
Printed in U.S.A.

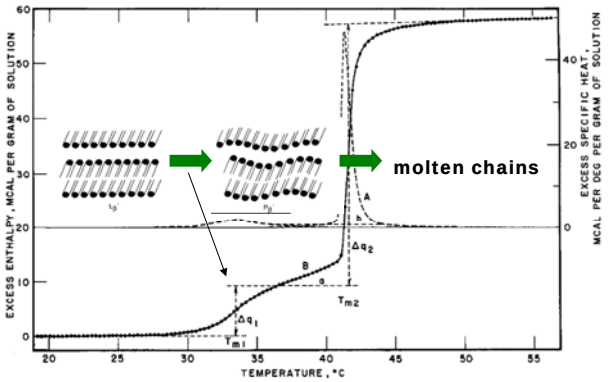

FIG. 1. The variation with temperature of the excess specific heat (*Curve A, right hand ordinates*) and the excess enthalpy (*Curve B, left hand ordinates*) during the gel to liquid crystal transition of dipalmitoyl L-α-lecithin in aqueous suspension at a lipid concentration of 3.88 mg per ml. The points on *Curve B* are the experimental data recorded digitally at 1-min intervals. The evaluation of the heat changes Δq_1 and Δq_2 is described in the text. The slope of the line after the upper transition corresponds to an apparent heat capacity increase, relative to the situation below the lower transition, of 13 cal deg^{-1} per mole of lipid.

microscopy

Optical microscopy
(typically:digital video enhanced microspcopy (VEM)

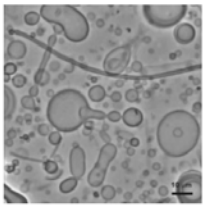

Transmission Electron Microscopy (TEM)
Cryo-TEM – rapid freezing of the sample (solution),

Plain TEM – works if the self-assembled structure survives dehydration

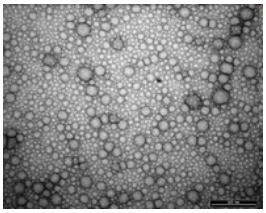

TEM image of
negatively stained vesicles
Wolfgang Meier, Basel

Pipette aspiration

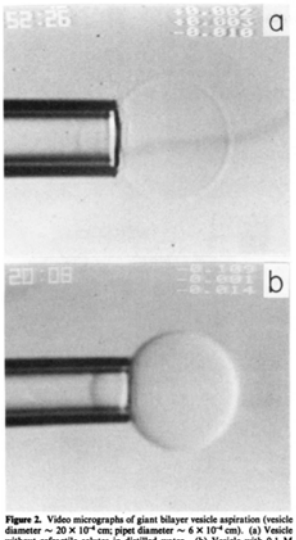

Figure 2. Video micrographs of giant bilayer vesicle aspiration (vesicle diameter ~ 20×10^{-4} cm; pipet diameter ~ 6×10^{-4} cm). (a) Vesicle without refractile solutes in distilled water. (b) Vesicle with 0.1 M sucrose inside and 0.1 M NaCl outside.

- vesicles are captured by a micropipette
- Transfer in other media is possible
- Pressure manipulation by applied suction pressure

→Access to physical properties of bilayer membranes (rigidity, interactions, thermal transitions, …)

advantage: projection length ~ change in total area (vesicle volume = constant at the applied pressures) small area changes are amplified and easily detectable

J. Phys. Chem. **1987**, *91*, 4219–4228

Physical Properties of Surfactant Bilayer Membranes: Thermal Transitions, Elasticity, Rigidity, Cohesion, and Colloidal Interactions

Evan Evans*
Pathology and Physics, University of British Columbia, Vancouver, B.C., Canada V6T 1W5
and David Needham
Mechanical Engineering and Material Science, Duke University, Durham, North Carolina 27706
(Received: February 2, 1987)

Pipette aspiration

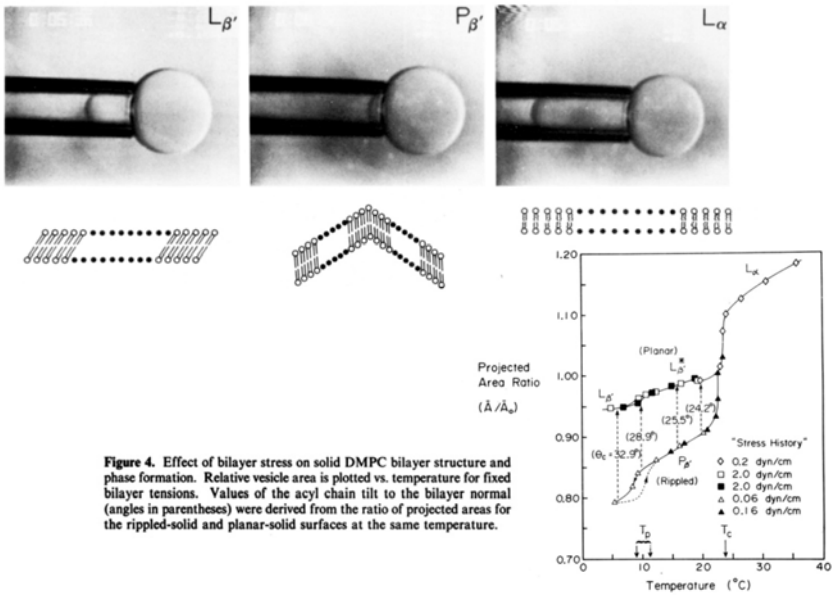

Figure 4. Effect of bilayer stress on solid DMPC bilayer structure and phase formation. Relative vesicle area is plotted vs. temperature for fixed bilayer tensions. Values of the acyl chain tilt to the bilayer normal (angles in parentheses) were derived from the ratio of projected areas for the rippled-solid and planar-solid surfaces at the same temperature.

Light Scattering

Measurement of radius of gyration R_g (static light scattering) and hydrodynamic radius R_h (dynamic light scattering) gives ρ-parameter:

$\rho = R_g/R_h$

for coils:	ρ = 1.73
for vesicles:	ρ = 1.0
for spheres (e.g micelles):	ρ = 0.775

Example (Helmut Schlaad, MPIKG)

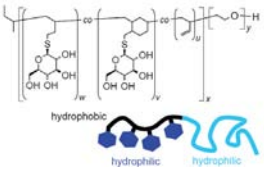

$w_{hydrophilic}$	$R_{h,0}$ / nm	$R_{g,0}$ / nm
0.76	550 ± 20	520 ± 20
0.58	270 ± 40	280 ± 30

DLS/SLS
0.025-0.1 wt % polymer in water

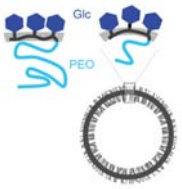

Basic functions of lipid membranes

- Barrier for passive diffusional motion of solutes (e.g. ions, sugar, protein, polysaccharides, nucleic acids, …
- Unique solvation environment for membrane proteins
- Internal organization of cells (compartmentalization)

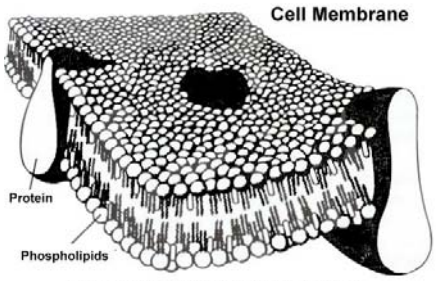

Human cell membrane formed by phospholipids

diffusional processes

Diffusional processes are always operable in living cells

Characterized by:

- flux (J)
- permeablity (P)
- concentration gradient (Δc)
- Diffusion coefficient (D)
- Partition coefficient (K)
  (describes partition od solute
  between bulk in membrane interior)
- Membrane thickness (d)

J = -P*Δc = -D*(dc/dz)
(Ficks 1st law)

P = D*K/d

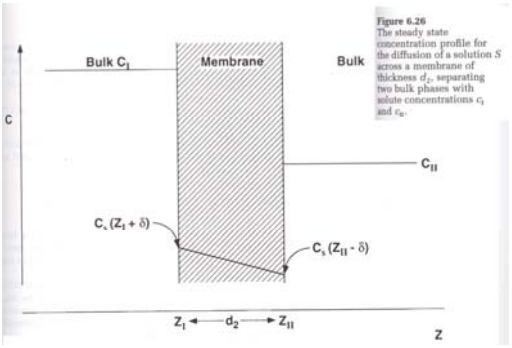

Figure 6.26
The steady state concentration profile for the diffusion of a solution S across a membrane of thickness d_2, separating two bulk phases with solute concentrations c_I and c_{II}.

For ions: additional electrostatic effects!

$$J(z) = -\frac{D}{RT} c(z) \frac{d\mu}{dz}$$

use of electrochemical potential yields correct description!

Diffusional processes

Experimental approach to investigate diffusion/transport:

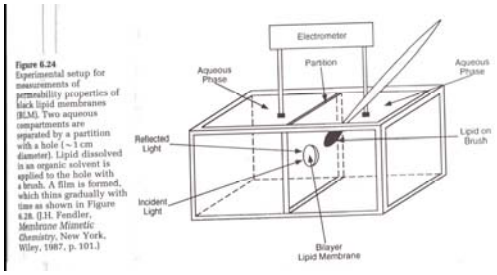

Figure 6.24
Experimental setup for measurements of permeability properties of black lipid membranes (BLM). Two aqueous compartments are separated by a partition with a hole (~1 cm diameter). Lipid dissolved in an organic solvent is applied to the hole with a brush. A film is formed, which thins gradually with time as shown in Figure 6.28. (J.H. Fendler, *Membrane Mimetic Chemistry*, New York, Wiley, 1987, p. 101.)

typical values for permeabilities of small solutes:

- P(water) ~ 5-100 x 10^{-6} m/s
- P(polar solutes, e.g. glucose, urea, glycerol) ~ 5-300 x 10^{-10} m/s
- P(small ions, e.g. Na+, K+, Cl-) ~ 1-100 x 10^{-14} m/s

Multilayer systems

hindered
Transport
($D_\perp$)

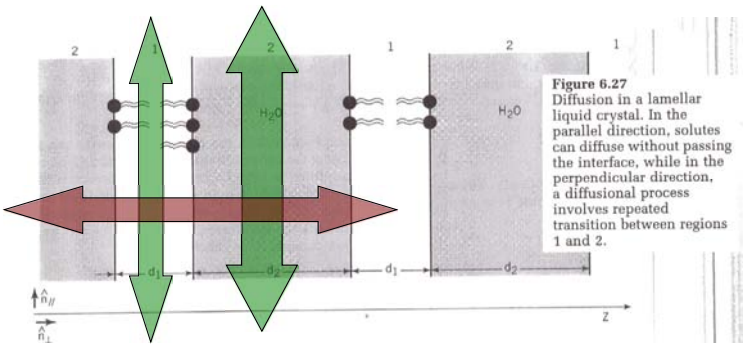

Figure 6.27
Diffusion in a lamellar liquid crystal. In the parallel direction, solutes can diffuse without passing the interface, while in the perpendicular direction, a diffusional process involves repeated transition between regions 1 and 2.

easy transport in parallel direction ($D_\parallel$)

Membrane proteins

typical membranes consist of 25-75 wt.% lipids, other species are: proteins, glycoproteins, lipoproteins, sugars…

proteins can be incorporated in a number of ways:

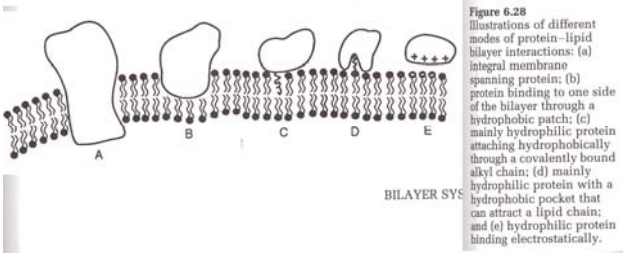

Figure 6.28
Illustrations of different modes of protein–lipid bilayer interactions: (a) integral membrane spanning protein; (b) protein binding to one side of the bilayer through a hydrophobic patch; (c) mainly hydrophilic protein attaching hydrophobically through a covalently bound alkyl chain; (d) mainly hydrophilic protein with a hydrophobic pocket that can attract a lipid chain; and (e) hydrophilic protein binding electrostatically.

Attention: proteins are inserted with a prescribed orientation!
cell membranes are assymetric, i.e. the surface of both sides are different (outer surface is often covered by sugars)

Protein mediated transmembrane transport

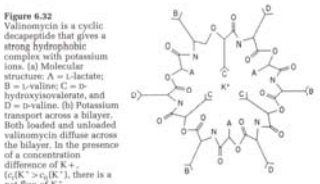

Figure 6.32
Valinomycin is a cyclic decapeptide that gives a strong hydrophobic complex with potassium ions. (a) Molecular structure: A = L-lactate; B = L-valine; C = D-hydroxyisovalerate, and D = D-valine. (b) Potassium transport across a bilayer. Both loaded and unloaded valinomycin diffuse across the bilayer. In the presence of a concentration difference of K+, ($c_i[K^+] > c_o[K^+]$), there is a net flux of K^+.

Pathway I for ion transport trough a membrane (carrier transport)

Pathway II for ion transport trough a membrane (channel transport)

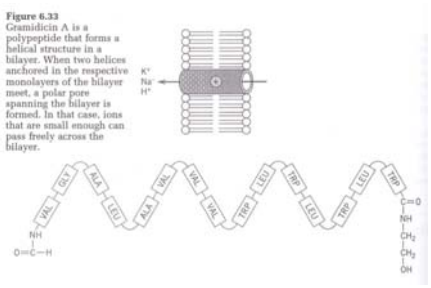

Figure 6.33
Gramidicin A is a polypeptide that forms a helical structure in a bilayer. When two helices anchored in the respective monolayers of the bilayer meet, a polar pore spanning the bilayer is formed. In that case, ions that are small enough can pass freely across the bilayer.

larger substances are transported by endo/exocytosis

compartmentalization

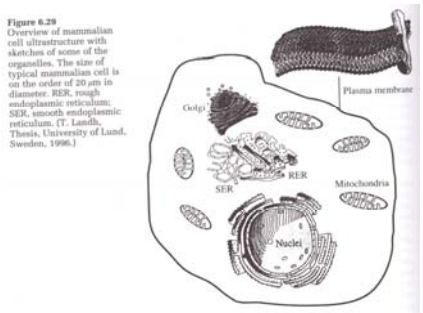

Figure 6.29
Overview of mammalian cell ultrastructure with sketches of some of the organelles. The size of typical mammalian cell is on the order of 20 μm in diameter. RER, rough endoplasmic reticulum; SER, smooth endoplasmic reticulum. (T. Landh, Thesis, University of Lund, Sweden, 1996.)

Generally:
Compartmentalization is required to provide the different unique enviroments for various processes

Typically: folding of membranes increases area/volume ratio

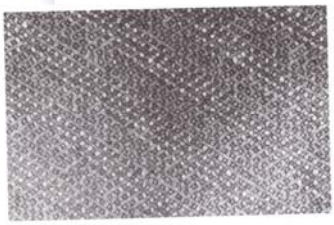

Figure 6.30
Electron micrograph of a patch of the smooth endoplasmic reticulum from a cell of a lemur, showing the membranes forming a structure of cubic symmetry. (Sisson and Fahrenbach, *Am. J. Anat.* **121**, 337 (1967).)

From Liposomes to Polymersomes

From Liposomes to Polymersomes

Universal validity of packing parameter:

low molecular weight surfactants → amphiphilic block copolymers

Advantage of high molecular weight surfactants (amphiphilic block copolymers)

- low CMC (critical micelle concentration)
  (e.g. CMC LMW surf.: 10^{-6} -10^{-7} M; CMC polymer: 10^{-9} M)
- adjustable hydrophobic-hydrophilic ratio (block length, segregation, solubility)
- adjustable rigidity (Gaussian coil → rigid rod)
- introduction of functions
- adjustable biodegradability, biocompatibility

→ less dynamic structures

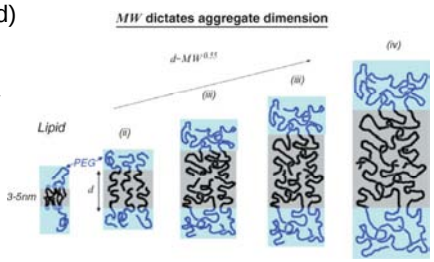

polymersomes

Eisenberg 1995: PS_{200}-*block*-poly acrylic $acid_8$ (water)

Nolte 1998: Stiffer hydrophobic block

poly(ethylene oxide)-*block*-poly(methylphenylsilane)

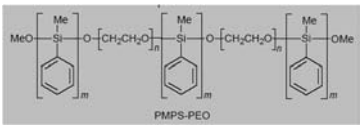

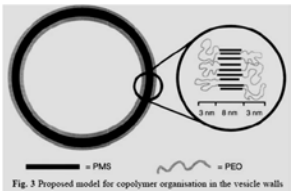

polymersomes

Responsive Systems

pH-degradable Systems (H. Schlaad, MPIKG)

pB_{216}-*block*-pMA_{29} ⟷ p-4Me4VP_{33}-*block*-pS_{211}

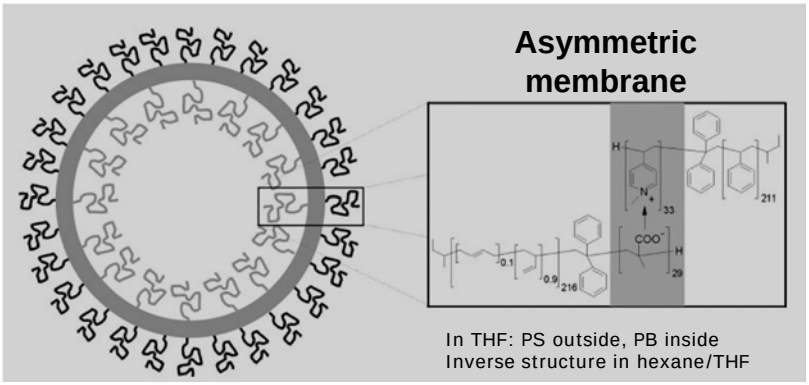

non self-assembled membranes

Other polymeric membranes

A variety of artificial membranes were developed for various separation/transport tasks

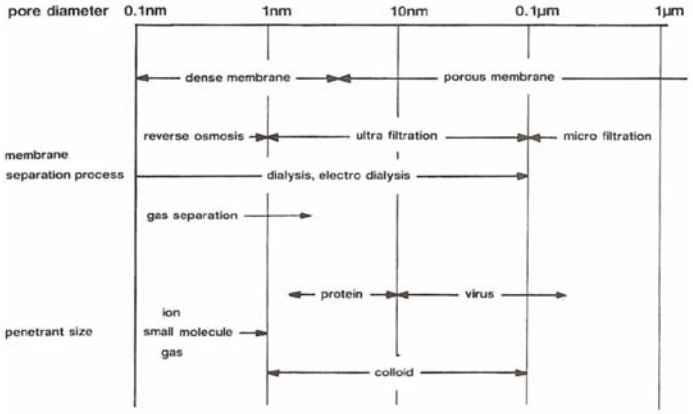

Proton Conduction Membranes

- Proton exchange membrane fuel cells (PEMFC):

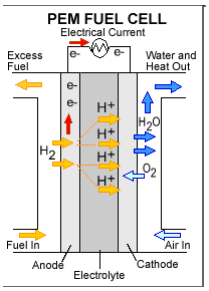

key part: **the membrane!**
good proton transport required! low crossover of fuel, etc…

→ microstructure has huge influence on performance

Proton Conduction Membranes

- Typically used: ionomer membranes (hydrophobic backbones with ionic side groups – strong polyelectrolytes which undergo microphase separation upon hydration – water channels!)

SAXS gives information about microstructure:

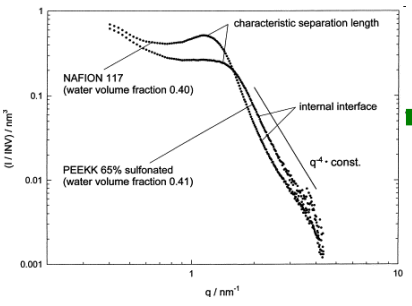

Journal of Membrane Science 185 (2001) 29–39

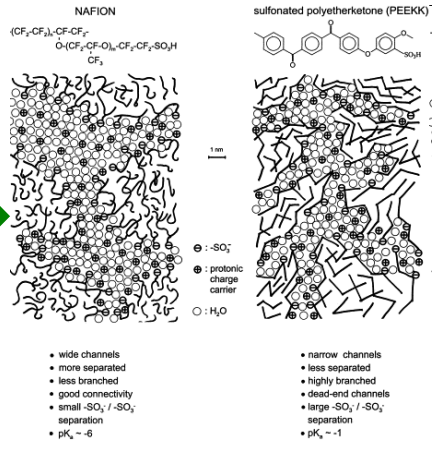

gas separation membranes

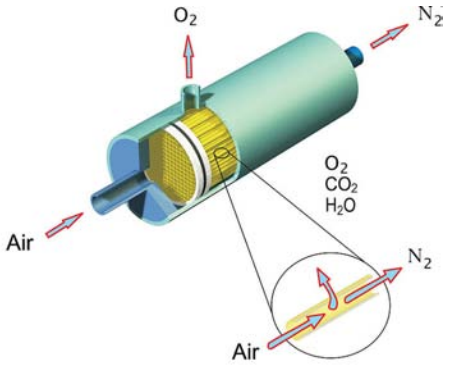

gas separation membranes

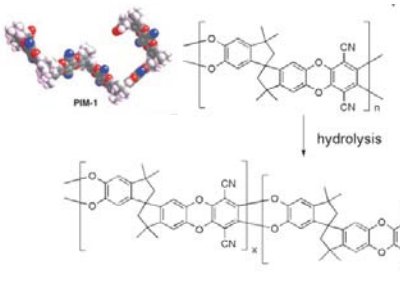

Microporous polymers (pore sizes ~0.7 nm) have high permeabilities but low selectivity

tuning of selectivity by polymer modification (e.g. hydrolysis of side groups)

polymers	carbon elemental analyses	*P* (Barrer)[a]					α[b]			
		O_2	N_2	He	H_2	CO_2	O_2/N_2	CO_2/N_2	He/N_2	H_2/N_2
PIM-1		1790	727	1368	3580	8310	2.5	11	1.9	4.9
120 °C, 1 h	74.29	534	162	616	1540	2543	3.3	16	3.8	9.5
120 °C, 2 h	73.10	351	100	484	1152	2060	3.5	21	4.9	12
120 °C, 3 h	71.67	201	48	260	630	1056	4.2	22	5.4	13
120 °C, 5 h	70.30	110	24	153	408	620	4.6	26	6.3	17

[a] Permeability coefficients measured at 25 °C and 50 psig feed pressure. One Barrer = 10^{-10} [cm^3(STP)·cm]/(cm^2·s·cmHg). [b] Ideal selectivity $\alpha = (P_a)/(P_b)$.

Macromolecules **2009**, *42*, 6038–6043
DOI: 10.1021/ma9009017

Literature

- „The Colloidal Domain“, by Evans and Wennerström
- and references therein